

Optimal key rates for quantum key distribution with partial source characterization

Margarida Pereira,^{1, 2, 3} Guillermo Currás-Lorenzo,^{1, 2, 3} and Mateus Araújo⁴

¹*Vigo Quantum Communication Center, University of Vigo, Vigo E-36310, Spain*

²*Escuela de Ingeniería de Telecomunicación, Department of Signal Theory and Communications, University of Vigo, Vigo E-36310, Spain*

³*atlanTTic Research Center, University of Vigo, Vigo E-36310, Spain*

⁴*Departamento de Física Teórica, Atómica y Óptica, Laboratory for Disruptive Interdisciplinary Science (LaDIS), Universidad de Valladolid, 47011 Valladolid, Spain*

Numerical security proofs based on conic optimization are known to deliver optimal secret-key rates, but so far they have mostly assumed that the emitted states are fully characterized. In practice, this assumption is unrealistic, since real devices inevitably suffer from imperfections and side channels that are extremely difficult to model in detail. Here, we extend conic-optimization methods to scenarios where only partial information about the emitted states is known, covering both prepare-and-measure and measurement-device-independent protocols. We demonstrate that our method outperforms state-of-the-art analytical and numerical approaches under realistic source imperfections, especially for protocols that use non-qubit encodings. These results advance numerical-based proofs towards a standard, implementation-ready framework for evaluating quantum key distribution protocols in the presence of source imperfections.

Introduction.—In principle, quantum key distribution (QKD) can achieve information-theoretic security, a much higher standard than any other cryptosystem. However, security proofs often assume ideal device models, while real implementations inevitably suffer from imperfections. These deviations can create security loopholes that allow Eve to gain information beyond what the security proof accounts for, potentially compromising QKD's security guarantees.

For example, standard security proofs of the well-known BB84 protocol [1] assume that Alice emits perfect qubit Pauli eigenstates, and that no information about her bit-and-basis choices is leaked to the eavesdropper, which is extremely difficult to satisfy in practice due to encoding imperfections and side channels. Significant progress has been made in developing analytical security proofs that incorporate such source imperfections [2–10]. In particular, analytical security proofs [5–9] have shown how to guarantee security under partial state characterization, i.e., when the emitted states are not completely known. For example, [9] requires only the knowledge that

$$\langle \phi_j | \rho_j | \phi_j \rangle \geq 1 - \epsilon_j, \quad (1)$$

where ρ_j is the actual state emitted by Alice when she selects setting j (e.g., for BB84, $j \in \{0_Z, 1_Z, 0_X, 1_X\}$), $|\phi_j\rangle$ is an arbitrary reference state, and ϵ_j bounds their deviation. However, these approaches often involve complicated derivations, as imperfections typically break the symmetries exploited by standard proofs, and can sometimes introduce loose bounds.

Numerical security proofs based on convex optimization [11–21] have recently emerged as a powerful alternative to analytical approaches. These can often achieve optimal or near-optimal key rates even for scenarios without such symmetries, which should in principle make them well-suited for handling imperfect sources. However, they

often assume a complete characterization of the emitted states [11–19], including all imperfections. This is a very unrealistic demand, since some imperfections are extremely difficult to characterize precisely.

It is then natural to ask whether numerical security proofs could incorporate partial state knowledge as analytical proofs do. Indeed, [20] has proposed a numerical approach that can bound the asymptotic key rate for prepare-and-measure and measurement-device-independent (MDI) type protocols given the knowledge in Eq. (1). However, the approach in [20] is not fully general, and it relies on phase-error estimation, which is not optimal for some protocols [22].

Thus, it is important to consider whether partial state characterization could be integrated into more general numerical techniques that directly optimize Eve's side information on Alice's key. Here, we introduce a simple yet effective method to achieve this. Specifically, we show how to extend the optimization framework in [18], which calculates *optimal* QKD key rates under full state characterization, to also calculate *optimal* QKD key rates under partial state characterization (i.e., the assumption in Eq. (1)). Moreover, we demonstrate that our method provides secret-key rates (SKR) surpassing those in [20], particularly for protocols employing non-qubit encodings.

Optimal key rates with full state characterization.—Consider a general prepare-and-measure QKD protocol in which, for each round, Alice sends known states $\{|\psi_j\rangle\}_j$, selected with probabilities $\{p_j\}_j$, where $j \in \{0, \dots, n-1\}$ and n is the total number of emitted states. To prove security, we can use an equivalent scenario in which Alice generates the source replacement state

$$|\Psi\rangle_{AA'} = \sum_{j=0}^{n-1} \sqrt{p_j} |j\rangle_A |\psi_j\rangle_{A'}, \quad (2)$$

where A is an ancillary system that Alice keeps in her possession, and A' is the photonic system sent through the quantum channel. Eve's collective attack can be described as an isometry $V_{A' \rightarrow BE}$, where B is the system that Eve resends to Bob, and E is Eve's ancillary system containing her side information. Since we are interested in the reduced state ρ_{AB} that Alice and Bob share after Eve's attack, we can define a CPTP map $\mathcal{E}_{A' \rightarrow B}$ that consists of first applying $V_{A' \rightarrow BE}$ and then tracing out system E . By doing so, we can write

$$\rho_{AB} = (\mathcal{I} \otimes \mathcal{E}_{A' \rightarrow B})(|\Psi\rangle\langle\Psi|_{AA'}). \quad (3)$$

Once Bob receives system B , he applies a POVM $\{\Gamma_k\}_k$ to the incoming state, where k denotes his measurement outcome.

The asymptotic key rate of a QKD protocol can be written as [12]

$$R_\infty = D(\mathcal{G}(\rho_{AB})\|\mathcal{Z}(\mathcal{G}(\rho_{AB}))) - p_{\text{pass}}\lambda_{\text{EC}}. \quad (4)$$

Here, D is the quantum relative entropy, \mathcal{G} and \mathcal{Z} are some completely positive maps defined in [12] that specify how Alice's sifted key is extracted, p_{pass} represents the probability that a round is used for sifted key generation, and λ_{EC} denotes the cost of error correction per sifted key bit. Note that the latter two terms are directly observable in the protocol, but the term $D(\mathcal{G}(\rho_{AB})\|\mathcal{Z}(\mathcal{G}(\rho_{AB})))$ cannot be directly calculated since the state ρ_{AB} is unknown (because Eve's map $\mathcal{E}_{A' \rightarrow B}$ is unknown). Therefore, this term needs to be optimized given the knowledge that is available to Alice and Bob. In particular, this is given by the convex optimization problem

$$\begin{aligned} & \min_{\rho_{AB}} D(\mathcal{G}(\rho_{AB})\|\mathcal{Z}(\mathcal{G}(\rho_{AB}))) \\ \text{s.t. } & \langle i|\rho_A|j\rangle = \sqrt{p_ip_j}\langle\psi_j|\psi_i\rangle, \quad \forall i, j \in \{0, \dots, n-1\}, \\ & \text{Tr}[(|j\rangle\langle j|_A \otimes \Gamma_k)\rho_{AB}] = p_j Y_{k|j}, \quad \forall j \in \{0, \dots, n-1\}, k, \\ & \rho_{AB} \succeq 0. \end{aligned} \quad (5)$$

The first constraint in Eq. (5) is equivalent to

$$\rho_A := \text{Tr}_B[\rho_{AB}] = \text{Tr}_{A'}[|\Psi\rangle\langle\Psi|_{AA'}], \quad (6)$$

and comes from the fact that Eve's map does not act on system A (see Eq. (3)), and therefore the marginal state on A must be the same before and after Eve applies her map. Note that this implies the constraint $\text{Tr}[\rho_{AB}] = 1$, which then should not be added explicitly, as redundant

constraints lead to numerical problems. The second constraint in Eq. (5) comes from Alice and Bob's observations during the protocol execution, where $Y_{k|j}$ refers to the conditional probability that Bob obtains outcome k given that Alice sends the state $|\psi_j\rangle$.

In [18], it is shown that a problem of the form in Eq. (5) can be reformulated as the following conic optimization problem

$$\begin{aligned} & \min_{h, \rho_{AB}} h \\ \text{s.t. } & \langle i|\rho_A|j\rangle = \sqrt{p_ip_j}\langle\psi_j|\psi_i\rangle, \quad \forall i, j \in \{0, \dots, n-1\}, \\ & \text{Tr}[(|j\rangle\langle j|_A \otimes \Gamma_k)\rho_{AB}] = p_j Y_{k|j}, \quad \forall j \in \{0, \dots, n-1\}, k, \\ & (h, \rho_{AB}) \in \mathcal{K}_{\text{QKD}}^{\widehat{\mathcal{G}}, \widehat{\mathcal{Z}}}, \end{aligned} \quad (7)$$

where $\mathcal{K}_{\text{QKD}}^{\widehat{\mathcal{G}}, \widehat{\mathcal{Z}}}$ is the QKD cone, defined as

$$\{(h, \rho) \in \mathbb{R} \times \mathbb{H}^d; \rho \succeq 0, h \geq -H(\widehat{\mathcal{G}}(\rho)) + H(\widehat{\mathcal{Z}}(\rho))\}, \quad (8)$$

where \mathbb{H}^d denotes the space of $d \times d$ complex Hermitian matrices, and $\widehat{\mathcal{G}}, \widehat{\mathcal{Z}}$ are obtained by performing facial reduction on \mathcal{G}, \mathcal{Z} and on the constraints of the problem (see [18] for more information). As shown in [18], a conic optimization problem of the form in Eq. (7) can be efficiently solved using interior point algorithms. In fact, the authors of [18] have developed a publicly available code to implement this optimization [23].

Optimal key rates with partial state characterization.—The approach described above works only when Alice's emitted states are fully known. Here, we show how to extend it to the scenario in which Alice's emitted states $\{\rho_j\}_j$ are only known to satisfy Eq. (1) for some known coefficients $\{\epsilon_j\}_j$, with $0 \leq \epsilon_j \leq 1$, and some known reference states $\{|\phi_j\rangle\}_j$.

First, we note that, given the knowledge in Eq. (1), one can assume without loss of generality that the emitted states have the form $\rho_j = |\psi_j\rangle\langle\psi_j|$, with

$$|\psi_j\rangle = \sqrt{1-\epsilon_j}|\phi_j\rangle + \sqrt{\epsilon_j}|\phi_j^\perp\rangle, \quad (9)$$

where $|\phi_j^\perp\rangle$ is an unknown state such that $\langle\phi_j^\perp|\phi_j\rangle = 0$. As proven in Appendix A (see also [20, Lemma 1]), any set of states $\{\rho_j\}_j$ satisfying Eq. (1) can be obtained by applying a CPTP map to a set of pure states $\{|\psi_j\rangle\}_j$ of the form in Eq. (9). This directly implies that, if security can be established for all such sets of pure states, then security is guaranteed for all sets of mixed states satisfying Eq. (1). Importantly, since pure states of the form in Eq. (9) themselves satisfy Eq. (1), this restriction does *not* constitute a relaxation. Therefore, the worst-case SKR under the knowledge in Eq. (1) can be expressed as the solution to the optimization problem

$$\begin{aligned}
& \min_{h, \rho_{AB}, \{|\phi_j^\perp\rangle\}_j} h \\
\text{s.t. } & \frac{\langle i|\rho_A|j\rangle}{\sqrt{p_i p_j}} = \sqrt{(1-\epsilon_i)(1-\epsilon_j)} \langle \phi_j|\phi_i\rangle + \sqrt{(1-\epsilon_i)\epsilon_j} \langle \phi_j^\perp|\phi_i\rangle + \sqrt{\epsilon_i(1-\epsilon_j)} \langle \phi_j|\phi_i^\perp\rangle + \sqrt{\epsilon_i\epsilon_j} \langle \phi_j^\perp|\phi_i^\perp\rangle, \quad \forall i, j, \\
& \text{Tr}[(|j\rangle\langle j|_A \otimes \Gamma_k)\rho_{AB}] = p_j Y_{k|j}, \quad \forall j, k, \\
& \langle \phi_j^\perp|\phi_j^\perp\rangle = 1, \quad \forall j, \\
& \langle \phi_j^\perp|\phi_j\rangle = 0, \quad \forall j, \\
& (h, \rho_{AB}) \in \mathcal{K}_{\text{QKD}}^{\hat{\mathcal{G}}, \hat{\mathcal{Z}}}.
\end{aligned} \tag{10}$$

Next, we show how to reformulate this as a conic problem. The key observation is that the optimization problem depends on the unknown states $\{|\phi_j^\perp\rangle\}_j$ only through their inner products with each other and with the known reference states $\{|\phi_j\rangle\}_j$. Therefore, instead of optimizing over the states themselves, we can optimize over a Gram matrix containing all these inner products, which converts the problem into a conic form. To be more precise, let G be the Gram matrix of the union of vector sets $\{|\phi_j\rangle\}_j \cup \{|\phi_j^\perp\rangle\}_j$, i.e., G is the $(2n \times 2n)$ positive semidefinite matrix:

$$G = \begin{pmatrix} \langle \phi_0|\phi_0\rangle & \langle \phi_0|\phi_1\rangle & \cdots & \langle \phi_0|\phi_0^\perp\rangle & \langle \phi_0|\phi_1^\perp\rangle & \cdots \\ \langle \phi_1|\phi_0\rangle & \langle \phi_1|\phi_1\rangle & \cdots & \langle \phi_1|\phi_0^\perp\rangle & \langle \phi_1|\phi_1^\perp\rangle & \cdots \\ \vdots & \vdots & \ddots & \vdots & \vdots & \ddots \\ \hline \langle \phi_0^\perp|\phi_0\rangle & \langle \phi_0^\perp|\phi_1\rangle & \cdots & \langle \phi_0^\perp|\phi_0^\perp\rangle & \langle \phi_0^\perp|\phi_1^\perp\rangle & \cdots \\ \langle \phi_1^\perp|\phi_0\rangle & \langle \phi_1^\perp|\phi_1\rangle & \cdots & \langle \phi_1^\perp|\phi_0^\perp\rangle & \langle \phi_1^\perp|\phi_1^\perp\rangle & \cdots \\ \vdots & \vdots & \ddots & \vdots & \vdots & \ddots \end{pmatrix}. \tag{11}$$

Note that some entries of this matrix are known, while others are not. More specifically, the known entries are: the entire upper left subblock (since the states $\{|\phi_j\rangle\}_j$ are known), all the diagonal entries (since all the states are normalized), and all the entries of the form $\langle \phi_j^\perp|\phi_j\rangle$ (which are equal to zero).

This is not a relaxation either, as the existence of a Gram matrix respecting these constraints is equivalent to the existence of a set of vectors with the required inner products. Thus, by introducing G as an optimization variable constrained by this known information, we can reformulate Eq. (10) as the conic optimization problem

$$\begin{aligned}
& \min_{h, \rho_{AB}, G} h \\
\text{s.t. } & \frac{\langle i|\rho_A|j\rangle}{\sqrt{p_i p_j}} = \sqrt{(1-\epsilon_i)(1-\epsilon_j)} G_{j,i} + \sqrt{(1-\epsilon_i)\epsilon_j} G_{j+n,i} + \sqrt{\epsilon_i(1-\epsilon_j)} G_{j,i+n} + \sqrt{\epsilon_i\epsilon_j} G_{j+n,i+n}, \quad \forall i, j, \\
& \text{Tr}[(|j\rangle\langle j|_A \otimes \Gamma_k)\rho_{AB}] = p_j Y_{k|j}, \quad \forall j, k, \\
& G_{i,j} = \langle \phi_i|\phi_j\rangle, \quad \forall i, j; i \neq j, \\
& G_{j+n,j} = 0, \quad \forall j, \\
& G_{j,j} = 1, \quad G_{j+n,j+n} = 1, \quad \forall j, \\
& (h, \rho_{AB}) \in \mathcal{K}_{\text{QKD}}^{\hat{\mathcal{G}}, \hat{\mathcal{Z}}}, \\
& G \succeq 0,
\end{aligned} \tag{12}$$

whose solution represents the exact SKR under partial state characterization, i.e., the knowledge in Eq. (1). Note that this is a conic optimization problem since the objective is linear and all constraints are either linear equalities or specify membership in convex cones (the QKD cone $\mathcal{K}_{\text{QKD}}^{\hat{\mathcal{G}}, \hat{\mathcal{Z}}}$ for (h, ρ_{AB}) and the positive semidefinite cone for G). Moreover, we remark that this conic optimization problem can be directly solved using the techniques in [18], and in particular, one can simply reuse the publicly available code in [23] after adding the new

constraints.

Note that when the reference states $\{|\phi_j\rangle\}_j$ are linearly dependent, no full rank G exists, which can cause issues when solving Eq. (12). As shown in Appendix B, this can be straightforwardly solved by constructing G using a basis for $\text{span}\{|\phi_j\rangle\}_j$, effectively reducing its dimension.

MDI-type protocols can be handled in an analogous manner: first reformulate them in the framework of [18], and then extend them with the partial state characterization constraints. We show this explicitly in Appendix C.

Numerical results.—Here, we apply our conic optimization approach to estimate the SKR for selected prepare-and-measure and MDI-type protocols with imperfect and partially characterized sources. To simulate the data that one would obtain in an actual implementation, we use standard channel models with detector efficiency $\eta_d = 0.73$, dark count probability $p_d = 10^{-6}$ and error correction inefficiency $f = 1.16$. For more information on the protocol modeling, see Appendix D.

We compare our results with the phase-error estimation method of [20], which provides an asymptotically optimal bound on the phase-error rate (see Appendix E for a proof of this claim). While phase-error estimation is widely used in QKD security proofs, it is known to underestimate the SKR in some situations [22]. Thus, our comparison allows us to evaluate when the phase-error approach remains near-optimal and when our direct optimization of Eve’s information provides an advantage.

We first consider the BB84 protocol and assume that the reference states are of the form

$$|\phi_j\rangle = \cos(\theta_j)|0_Z\rangle + \sin(\theta_j)|1_Z\rangle. \quad (13)$$

Here, $\theta_j = (1 + \delta/\pi)\varphi_j/2$, with $\varphi_j \in \{0, \pi, \pi/2, 3\pi/2\}$ and $\delta \in [0, \pi]$, for $j \in \{0, 1, 2, 3\}$, which corresponds to the bit-and-basis values $\{0_Z, 1_Z, 0_X, 1_X\}$. The actual emitted states ρ_j satisfy the partial characterization constraint in Eq. (1) with $\epsilon_j = \epsilon \forall j$. In this model, δ quantifies the magnitude of characterized state preparation flaws within the qubit space (e.g., polarization rotation errors), while ϵ incorporates uncharacterized imperfections such as information leakage through additional degrees of freedom or side channels [9]. For Bob’s measurement, we consider a standard BB84 setup with an active basis choice. Since numerical methods require Bob’s POVM to act on a finite-dimensional system while optical detectors act on an infinite-dimensional Fock space, we apply the qubit squashing map [24, 25]. For simplicity, we consider that all of Bob’s detectors have the same efficiencies and dark count rates, which can be treated as channel-induced losses and noise, respectively [26]. Scenarios in which the efficiencies and dark count rates of Bob’s detectors differ (in a partially characterized way) can be incorporated into our optimization problem by applying the tools in [26] in combination with the flag-state squasher [27].

Figure 1 shows the SKR as a function of distance for $\delta = 0.14$ and different values of ϵ . The solid lines represent our conic optimization approach, while the dashed lines show the phase-error estimation results from [20]. We observe that both methods give nearly identical results across all parameter regimes. The phase-error approach is known to be asymptotically optimal for ideal BB84, and our results suggest it remains near-optimal even with source imperfections, at least under our imperfections model. Furthermore, since our conic optimization results coincide with those of the phase-error method, which was already shown in [20] to reproduce

the analytical key rates of [9], these findings demonstrate that [9] is essentially optimal for this scenario, at least in the asymptotic regime—an interesting result, since analytical bounds used to handle imperfect and partially characterized sources can often introduce looseness.

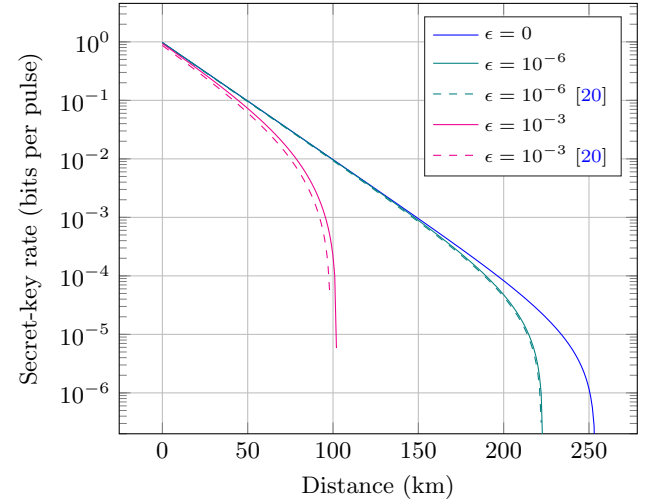


Figure 1. Secret-key rate (logarithmic scale) as a function of distance for the BB84 protocol with $\delta = 0.14$ and different values of ϵ . The solid lines correspond to our conic optimization approach while the dashed lines correspond to the phase-error estimation method of [20]. The curve obtained for $\epsilon = 0$ when using the latter analysis is omitted as its visually indistinguishable from that obtained when using our approach.

Next, we analyze a coherent-light-based MDI protocol introduced in [7], which can be regarded as a simplified version of twin-field QKD [28]. This scheme employs a very different encoding from BB84: instead of qubit states, each user emits two coherent states with opposite phases (for key generation) plus a vacuum state (for parameter estimation). Since phase-error estimation was developed specifically for qubit-based protocols like BB84, this coherent-state encoding is a good benchmark to evaluate whether our direct optimization method provides advantages for protocols whose encoding differs significantly from BB84.

In this case, the joint reference states of Alice and Bob are

$$|\phi_{ij}\rangle = |\phi_i\rangle \otimes |\phi_j\rangle, \quad \text{for } i, j \in \{0, 1, 2\}, \quad (14)$$

where the individual states are defined as

$$|\phi_0\rangle = |\alpha\rangle, \quad |\phi_1\rangle = |-\alpha e^{i\delta}\rangle \quad \text{and} \quad |\phi_2\rangle = |\text{vac}\rangle, \quad (15)$$

with α denoting the amplitude of the coherent state and δ the characterized state preparation flaws. We consider that the joint emitted states $\rho_{ij} = \rho_i \otimes \rho_j$ satisfy the partial characterization constraint

$$\langle\phi_{ij}|\rho_{ij}|\phi_{ij}\rangle \geq (1 - \epsilon)^2, \quad \forall i, j, \quad (16)$$

where the squared term comes from the fact that this constraint could be obtained by combining two individual constraints of the form in Eq. (1), one for each user.

Figure 2 presents the SKR for this MDI-type protocol with $\delta = 0.14$ and various values of ϵ . In this case, we observe a clear performance gap between our conic optimization (solid lines) and the phase-error approach (dashed lines) [20]. Our method consistently yields higher SKR values, and the advantage becomes more pronounced at longer distances and for smaller ϵ . For instance, at $\epsilon = 0$, our approach extends the maximum achievable distance by more than 10 km compared to the phase-error estimation method. We have performed additional simulations with $\delta = 0$ and $p_d = 10^{-4}$, and observed that, in this regime, our approach also outperforms that in [20] (see Section F for more details). We note that, in the asymptotic regime, [20] already outperforms considerably the tightest analytical proof available for this protocol [9].

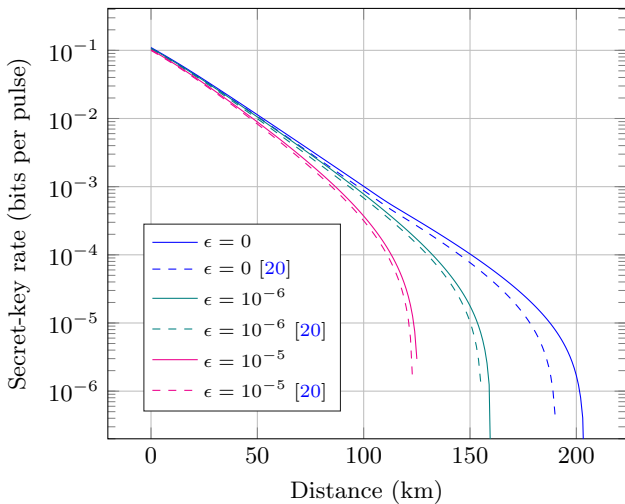


Figure 2. Secret-key rate rate (logarithmic scale) as a function of distance for the coherent-light-based MDI-type protocol introduced in [7], with $\delta = 0.14$ and different values of ϵ . The parameter α has been optimized for each distance point, taking values in the range $[0.03, 0.5]$. All computations were performed with double floats for increased precision and stability.

Conclusion. In this work, we introduced a conic optimization approach that extends the framework of [18] from full to partial state characterization, thereby providing *optimal* key rates for general prepare-and-measure and MDI-type protocols under realistic conditions. This method directly optimizes Eve’s side information and overcomes the limitations of [20], which also considered partial characterization but relied on phase-error estimation and lacked full generality [29]. For qubit-based protocols such as BB84, our approach achieves nearly identical performance to the phase-error estimation method, showing that the latter is nearly optimal in this setting. In contrast, for protocols with non-qubit encodings, such

as a coherent-light-based MDI protocol, our approach offers a clear improvement with respect to that in [20]. These results underscore the potential of conic optimization for analyzing realistic source imperfections and establishing security across a broad range of QKD protocols while achieving high performance.

A natural next step is applying our framework to decoy-state QKD [30–32]. For perfectly phase-randomized weak coherent sources, this is straightforward: the standard decoy analysis provides upper and lower bounds on the single-photon yields, which can be incorporated into our optimization problem by replacing the corresponding equality constraints with inequalities. However, realistic imperfections and side channels in intensity modulation and phase randomization prevent signals from being modeled as ideal photon-number mixtures, invalidating this simple approach. While [21] has recently shown how to incorporate some of these imperfections into numerical-based proofs, developing a general framework that handles both bit-and-basis encoding imperfections and decoy imperfections in a partially uncharacterized manner remains an important open problem. We anticipate that the tools introduced in our work will prove valuable in addressing this challenge.

Another important challenge is the extension of our approach to the finite-key regime. For this, one could employ established methods such as the postselection technique [33, 34] or the generalized entropy accumulation theorem [35], which would require incorporating statistical fluctuations into the constraints but would largely preserve the structure of our optimization. However, more recent approaches based on the marginal-constrained entropy accumulation theorem [36] in combination with optimization over Rényi entropies [21] provide significantly tighter finite-key estimates. While adapting our framework to this setting would require extending the conic formulation to handle Rényi rather than von Neumann entropies, such an extension is expected to be feasible and would provide a promising route towards tight and practical finite-key security guarantees.

Code availability. The code to reproduce our results is available at https://github.com/araujoms/qkd_partial_characterization.

Acknowledgements. We thank Matej Pivoluska for the idea to rephrase our justification in Appendix A in terms of source mapping and for discussions regarding the extension of our framework to decoy-state protocols. Also, we thank Marcos Curty and Álvaro Navarrete for valuable discussions. The research of M.A. was supported by the Spanish Agencia Estatal de Investigación, Grant No. RYC2023-044074-I, by the Q-CAYLE project, funded by the European Union-Next Generation UE/MICIU/Plan de Recuperación, Transformación y Resiliencia/Junta de Castilla y León (PRTC17.11), and also by the Department of Education of the Junta de Castilla y León and FEDER Funds (Reference: CLU-2023-1-05). M.P. and G.C.-

L. acknowledge support from the Galician Regional Government (consolidation of research units: atlanTic), the Spanish Ministry of Economy and Competitiveness (MINECO), the Fondo Europeo de Desarrollo Regional (FEDER) through the grant No. PID2020-118178RB-C21, MICIN with funding from the European Union NextGenerationEU (PRTRC17.I1) and the Galician Regional Government with own funding through the “Planes Complementarios de I+D+I con las Comunidades Autonomas” in Quantum Communication, the “Hub Nacional de Excelencia en Comunicaciones Cuanticas” funded by the Spanish Ministry for Digital

Transformation and the Public Service and the European Union NextGenerationEU, the European Union’s Horizon Europe Framework Programme under the Marie Skłodowska-Curie Grant No. 101072637 (Project QSI), the project “Quantum Security Networks Partnership” (QSNP, grant agreement No 101114043) and the European Union via the European Health and Digital Executive Agency (HADEA) under the Project QuTechSpace (grant 101135225). G.C.-L. acknowledges funding from the European Union’s Horizon Europe research and innovation programme under the Marie Skłodowska-Curie Postdoctoral Fellowship grant agreement No. 101149523.

[1] C. H. Bennett and G. Brassard, Quantum cryptography: Public key distribution and coin tossing, in *Proceedings of IEEE International Conference on Computers, Systems, and Signal Processing* (1984) pp. 175–179.

[2] D. Gottesman, H.-K. Lo, N. Lütkenhaus, and J. Preskill, Security of quantum key distribution with imperfect devices, *Quantum Inf. Comput.* **4**, 325 (2004).

[3] H.-K. Lo and J. Preskill, Security of quantum key distribution using weak coherent states with nonrandom phases, *Quantum Inf. Comput.* **7**, 431 (2007).

[4] K. Tamaki, M. Curty, G. Kato, H.-K. Lo, and K. Azuma, Loss-tolerant quantum cryptography with imperfect sources, *Phys. Rev. A* **90**, 052314 (2014).

[5] M. Pereira, M. Curty, and K. Tamaki, Quantum key distribution with flawed and leaky sources, *npj Quantum Inf* **5**, 62 (2019).

[6] M. Pereira, G. Kato, A. Mizutani, M. Curty, and K. Tamaki, Quantum key distribution with correlated sources, *Sci. Adv.* **6**, eaaz4487 (2020).

[7] Á. Navarrete, M. Pereira, M. Curty, and K. Tamaki, Practical Quantum Key Distribution That is Secure Against Side Channels, *Phys. Rev. Applied* **15**, 034072 (2021).

[8] M. Pereira, G. Currás-Lorenzo, Á. Navarrete, A. Mizutani, G. Kato, M. Curty, and K. Tamaki, Modified BB84 quantum key distribution protocol robust to source imperfections, *Phys. Rev. Res.* **5**, 023065 (2023).

[9] G. Currás-Lorenzo, M. Pereira, G. Kato, M. Curty, and K. Tamaki, Security of high-speed quantum key distribution with imperfect sources (2025), [arXiv:2305.05930 \[quant-ph\]](https://arxiv.org/abs/2305.05930).

[10] X.-B. Wang, X.-L. Hu, and Z.-W. Yu, Practical Long-Distance Side-Channel-Free Quantum Key Distribution, *Phys. Rev. Applied* **12**, 054034 (2019).

[11] P. J. Coles, E. M. Metodiev, and N. Lütkenhaus, Numerical approach for unstructured quantum key distribution, *Nat Commun* **7**, 11712 (2016).

[12] A. Winick, N. Lütkenhaus, and P. J. Coles, Reliable numerical key rates for quantum key distribution, *Quantum* **2**, 77 (2018).

[13] Y. Wang, I. W. Primaatmaja, E. Lavie, A. Varvitsiotis, and C. C. W. Lim, Characterising the correlations of prepare-and-measure quantum networks, *npj Quantum Inf* **5**, 1 (2019).

[14] I. W. Primaatmaja, E. Lavie, K. T. Goh, C. Wang, and C. C. W. Lim, Versatile security analysis of measurement-device-independent quantum key distribution, *Phys. Rev. A* **99**, 062332 (2019).

[15] H. Hu, J. Im, J. Lin, N. Lütkenhaus, and H. Wolkowicz, Robust Interior Point Method for Quantum Key Distribution Rate Computation, *Quantum* **6**, 792 (2022).

[16] H. Zhou, T. Sasaki, and M. Koashi, Numerical method for finite-size security analysis of quantum key distribution, *Phys. Rev. Res.* **4**, 033126 (2022).

[17] M. Araújo, M. Huber, M. Navascués, M. Pivoluska, and A. Tavakoli, Quantum key distribution rates from semidefinite programming, *Quantum* **7**, 1019 (2023).

[18] A. G. Lorente, P. V. Parellada, M. Castillo-Celeita, and M. Araújo, Quantum key distribution rates from non-symmetric conic optimization, *Quantum* **9**, 1657 (2025).

[19] K. He, J. Saunderson, and H. Fawzi, Exploiting structure in quantum relative entropy programs (2024), [arXiv:2407.00241 \[quant-ph\]](https://arxiv.org/abs/2407.00241).

[20] G. Currás-Lorenzo, Á. Navarrete, J. Núñez-Bon, M. Pereira, and M. Curty, Numerical security analysis for quantum key distribution with partial state characterization, *Quantum Sci. Technol.* **10**, 035031 (2025).

[21] L. Kamin, J. Burniston, and E. Y.-Z. Tan, Rényi security framework against coherent attacks applied to decoy-state QKD (2025), [arXiv:2504.12248 \[quant-ph\]](https://arxiv.org/abs/2504.12248).

[22] T. Matsuura, S. Yamano, Y. Kuramochi, T. Sasaki, and M. Koashi, Asymptotically tight security analysis of quantum key distribution based on universal source compression (2025), [arXiv:2504.07356 \[quant-ph\]](https://arxiv.org/abs/2504.07356).

[23] *ConicQKD.jl: Implementation of the QKD cone for quantum key distribution rate optimization* (2025).

[24] N. J. Beaudry, T. Moroder, and N. Lütkenhaus, Squashing Models for Optical Measurements in Quantum Communication, *Phys. Rev. Lett.* **101**, 093601 (2008).

[25] O. Gittsovich, N. J. Beaudry, V. Narasimhachar, R. R. Alvarez, T. Moroder, and N. Lütkenhaus, Squashing model for detectors and applications to quantum-key-distribution protocols, *Phys. Rev. A* **89**, 012325 (2014).

[26] S. Nahar, D. Tupkary, and N. Lütkenhaus, Imperfect detectors for adversarial tasks with applications to quantum key distribution (2025), [arXiv:2503.06328 \[quant-ph\]](https://arxiv.org/abs/2503.06328).

[27] Y. Zhang, P. J. Coles, A. Winick, J. Lin, and N. Lütkenhaus, Security proof of practical quantum key distribution with detection-efficiency mismatch, *Phys. Rev. Research* **3**, 013076 (2021).

[28] M. Lucamarini, Z. Yuan, J. Dynes, and A. Shields, Overcoming the rate–distance limit of quantum key distribution

tion without quantum repeaters, *Nature* **557**, 400 (2018).

[29] When applied to prepare-and-measure protocols, the approach in [20] requires that Bob performs two POVMs with the same overall detection efficiency, which only makes sense in BB84-type protocols with an active measurement basis choice. Thus, the approach in [20] is not directly applicable, for example, to the six-state protocol, or even to BB84 with a passive measurement basis choice. Our approach does not have these limitations, and can be applied to general prepare-and-measure protocols.

[30] W.-Y. Hwang, Quantum key distribution with high loss: Toward global secure communication, *Physical Review Letters* **91**, 057901 (2003).

[31] H.-K. Lo, X. Ma, and K. Chen, Decoy State Quantum Key Distribution, *Phys. Rev. Lett.* **94**, 230504 (2005).

[32] X.-B. Wang, Beating the Photon-Number-Splitting Attack in Practical Quantum Cryptography, *Phys. Rev. Lett.* **94**, 230503 (2005).

[33] M. Christandl, R. König, and R. Renner, Postselection Technique for Quantum Channels with Applications to Quantum Cryptography, *Phys. Rev. Lett.* **102**, 020504 (2009).

[34] S. Nahar, D. Tukary, Y. Zhao, N. Lütkenhaus, and E. Y.-Z. Tan, Postselection Technique for Optical Quantum Key Distribution with Improved de Finetti Reductions, *PRX Quantum* **5**, 040315 (2024).

[35] T. Metger, O. Fawzi, D. Sutter, and R. Renner, Generalised entropy accumulation, in *2022 IEEE 63rd Annual Symposium on Foundations of Computer Science (FOCS)* (2022) pp. 844–850.

[36] A. Arqand and E. Y.-Z. Tan, Marginal-constrained entropy accumulation theorem (2025), [arXiv:2502.02563](https://arxiv.org/abs/2502.02563) [quant-ph].

Appendix A: Justification for Eq. (9)

Here, we provide a rigorous justification for our assumption in Eq. (9) of the main text. We note that this is essentially the same justification as in [20, Lemma 1] (see also a similar previous result in [9]) but rephrased in the language of *source mapping*.

Lemma 1. *Let $\{\rho_j\}_j$ with $j \in \{0, 1, \dots, n-1\}$ be a set of states satisfying*

$$\langle \phi_j | \rho_j | \phi_j \rangle \geq 1 - \epsilon_j, \quad \forall j, \quad (\text{A1})$$

for a fixed set of pure states $\{|\phi_j\rangle\}_j$. Then there exist a CPTP map Φ and pure states $\{|\psi_j\rangle\}_j$ of the form

$$|\psi_j\rangle = \sqrt{1 - \epsilon_j} |\phi_j\rangle + \sqrt{\epsilon_j} |\phi_j^\perp\rangle, \quad (\text{A2})$$

where $\langle \phi_j^\perp | \phi_j \rangle = 0$, such that

$$\rho_j = \Phi(|\psi_j\rangle\langle\psi_j|), \quad \forall j. \quad (\text{A3})$$

As a consequence, for any prepare-and-measure QKD protocol, if security can be established for all pure state preparations $\{|\psi_j\rangle\}_j$ satisfying Eq. (A2), then security is guaranteed for all mixed state preparations $\{\rho_j\}_j$ satisfying Eq. (A1).

Proof. Consider a fixed set $\{\rho_j\}_j$ satisfying Eq. (A1). By Uhlmann's theorem, for each j there exists a purification $|\psi_j''\rangle_{aS}$ of ρ_j such that

$$|\langle \phi_j | \psi_j'' \rangle_{aS}|^2 = \langle \phi_j | \rho_j | \phi_j \rangle \geq 1 - \epsilon_j, \quad (\text{A4})$$

where $|\phi_j\rangle_{aS} := |\phi_j\rangle |0\rangle_S$ with S denoting an ancillary system. Without loss of generality, Eq. (A4) implies that $|\psi_j''\rangle_{aS}$ can be expressed as

$$|\psi_j''\rangle_{aS} = e^{i\varphi_j} \left(\sqrt{1 - \epsilon'_j} |\phi_j\rangle_{aS} + \sqrt{\epsilon'_j} |\phi_j'^\perp\rangle_{aS} \right), \quad (\text{A5})$$

where $0 \leq \epsilon'_j \leq \epsilon_j$, $\varphi_j \in [0, 2\pi)$, and $\langle \phi_j'^\perp | \phi_j \rangle_{aS} = 0$. Moreover, we can eliminate the global phase by defining

$$|\psi_j'\rangle_{aS} = e^{-i\varphi_j} |\psi_j''\rangle_{aS} = \sqrt{1 - \epsilon'_j} |\phi_j\rangle_{aS} + \sqrt{\epsilon'_j} |\phi_j'^\perp\rangle_{aS}, \quad (\text{A6})$$

which is also a purification of ρ_j .

Next, we show that ϵ'_j can be replaced by ϵ_j by introducing a fictitious system F . Consider the states $\{|\psi_j\rangle_{aSF}\}_j$ defined as

$$|\psi_j\rangle_{aSF} = |\psi_j'\rangle_{aS} \otimes \left[\sqrt{\frac{1 - \epsilon_j}{1 - \epsilon'_j}} |0\rangle_F + \sqrt{1 - \frac{1 - \epsilon_j}{1 - \epsilon'_j}} |1\rangle_F \right], \quad (\text{A7})$$

where $\{|0\rangle_F, |1\rangle_F\}$ is an orthonormal basis for system F . This can be rewritten as

$$|\psi_j\rangle_{aSF} = \sqrt{1 - \epsilon_j} |\phi_j\rangle_{aSF} + \sqrt{\epsilon_j} |\phi_j^\perp\rangle_{aSF}, \quad (\text{A8})$$

where $|\phi_j\rangle_{aSF} := |\phi_j\rangle_{aS} |0\rangle_F$ and

$$|\phi_j^\perp\rangle_{aSF} = \frac{\sqrt{\epsilon_j - \epsilon'_j}}{\sqrt{\epsilon_j}} |\phi_j\rangle_{aS} |1\rangle_F + \frac{\sqrt{\epsilon'_j}}{\sqrt{\epsilon_j}} |\phi_j'^\perp\rangle_{aS} \otimes \left[\sqrt{\frac{1 - \epsilon_j}{1 - \epsilon'_j}} |0\rangle_F + \sqrt{\frac{\epsilon_j - \epsilon'_j}{1 - \epsilon'_j}} |1\rangle_F \right] \quad (\text{A9})$$

is a normalized state orthogonal to $|\phi_j\rangle_{aSF}$.

Finally, we define the CPTP map $\Phi(\cdot) = \text{Tr}_{SF}(\cdot)$. By construction,

$$\rho_j = \Phi(|\psi_j\rangle\langle\psi_j|_{aSF}), \quad (\text{A10})$$

i.e., Eq. (A3), as required.

Security implication. Consider a fixed pair of sets $\{\rho_j\}_j$ and $\{|\psi_j\rangle\}_j$ related by Eq. (A10). Since generating $\{\rho_j\}_j$ is equivalent to first preparing $\{|\psi_j\rangle\}_j$ and then applying Φ , the map Φ can be absorbed into Eve's attack. Consequently, any protocol secure against all attacks when Alice prepares $\{|\psi_j\rangle\}_j$ remains secure when she prepares $\{\rho_j\}_j$ (see, e.g., [34, Lemma 8] for a formal proof of this statement). Since we have shown that every set $\{\rho_j\}_j$ satisfying Eq. (A1) can be obtained via Eq. (A10) from some set $\{|\psi_j\rangle\}_j$ of the form in Eq. (A2), it follows that proving security for all such pure state preparations guarantees security for all mixed state preparations satisfying Eq. (A1). \square

We remark that an equivalent result can also be derived for MDI-type protocols to justify our assumption in Eq. (C8) given the knowledge in Eq. (C7).

Appendix B: Handling linearly dependent reference states

When the reference states $\{|\phi_j\rangle\}_j$ for $j \in \{0, \dots, n-1\}$, with n denoting the number of emitted states, are linearly dependent, the Gram matrix G defined in the main text cannot have full rank, which may lead to numerical instability when solving Eq. (12). Here, we show how to reformulate the problem using a basis for $\text{span}\{|\phi_j\rangle\}_j$, effectively reducing the dimension of the Gram matrix. Let $n_{\text{dim}} = \dim(\text{span}\{|\phi_j\rangle\}_j) \leq n$ be the dimension of the subspace spanned by the reference states. We construct an orthonormal basis $\{|l\rangle\}_{l=0}^{n_{\text{dim}}-1}$ for this subspace, allowing us to express each reference state as

$$|\phi_j\rangle = \sum_{l=0}^{n_{\text{dim}}-1} c_l^{(j)} |l\rangle, \quad (\text{B1})$$

where the coefficients $c_l^{(j)} = \langle l|\phi_j\rangle$ are known since both $\{|l\rangle\}_l$ and $\{|\phi_j\rangle\}_j$ are known. Now, instead of constructing the Gram matrix using the states $\{|\phi_j\rangle\}_j \cup \{|\phi_j^\perp\rangle\}_j$ as in the main text, we construct a reduced Gram matrix G using the basis states $\{|l\rangle\}_l \cup \{|\phi_j^\perp\rangle\}_j$. This results in a $(n_{\text{dim}} + n) \times (n_{\text{dim}} + n)$ positive semidefinite matrix:

$$G = \begin{pmatrix} \langle 0|0\rangle & \cdots & \langle 0|n_{\text{dim}}-1\rangle & | & \langle 0|\phi_0^\perp\rangle & \cdots & \langle 0|\phi_{n-1}^\perp\rangle \\ \vdots & \ddots & \vdots & | & \vdots & \ddots & \vdots \\ \langle n_{\text{dim}}-1|0\rangle & \cdots & \langle n_{\text{dim}}-1|n_{\text{dim}}-1\rangle & | & \langle n_{\text{dim}}-1|\phi_0^\perp\rangle & \cdots & \langle n_{\text{dim}}-1|\phi_{n-1}^\perp\rangle \\ \langle \phi_0^\perp|0\rangle & \cdots & \langle \phi_0^\perp|n_{\text{dim}}-1\rangle & | & \langle \phi_0^\perp|\phi_0^\perp\rangle & \cdots & \langle \phi_0^\perp|\phi_{n-1}^\perp\rangle \\ \vdots & \ddots & \vdots & | & \vdots & \ddots & \vdots \\ \langle \phi_{n-1}^\perp|0\rangle & \cdots & \langle \phi_{n-1}^\perp|n_{\text{dim}}-1\rangle & | & \langle \phi_{n-1}^\perp|\phi_0^\perp\rangle & \cdots & \langle \phi_{n-1}^\perp|\phi_{n-1}^\perp\rangle \end{pmatrix}. \quad (\text{B2})$$

The known entries of this matrix are: the upper left $n_{\text{dim}} \times n_{\text{dim}}$ block, which equals $I_{n_{\text{dim}}}$ (since $\{|l\rangle\}_l$ is orthonormal), and the diagonal entries $G_{j+n_{\text{dim}}, j+n_{\text{dim}}} = 1$ for all j (since all states are normalized). Additionally, the orthogonality constraint $\langle \phi_j^\perp | \phi_j \rangle = 0$ translates to

$$\sum_{l=0}^{n_{\text{dim}}-1} G_{j+n_{\text{dim}}, l} c_l^{(j)} = 0, \quad \forall j. \quad (\text{B3})$$

Using this reduced Gram matrix, we can express the required inner products as:

$$\begin{aligned} \langle \phi_i | \phi_j \rangle &= \sum_{l=0}^{n_{\text{dim}}-1} \overline{c_l^{(i)}} c_l^{(j)} \quad (\text{known}), \\ \langle \phi_i^\perp | \phi_j \rangle &= \sum_{l=0}^{n_{\text{dim}}-1} G_{i+n_{\text{dim}}, l} c_l^{(j)}, \\ \langle \phi_i | \phi_j^\perp \rangle &= \sum_{l=0}^{n_{\text{dim}}-1} \overline{c_l^{(i)}} G_{l, j+n_{\text{dim}}}, \\ \langle \phi_i^\perp | \phi_j^\perp \rangle &= G_{i+n_{\text{dim}}, j+n_{\text{dim}}}. \end{aligned} \quad (\text{B4})$$

The conic optimization problem then becomes

$$\begin{aligned}
& \min_{h, \rho_{AB}, G} h \\
\text{s.t. } & \frac{\langle i | \rho_A | j \rangle}{\sqrt{p_i p_j}} = \sqrt{(1 - \epsilon_i)(1 - \epsilon_j)} \sum_{l=0}^{n_{\text{dim}}-1} \overline{c_l^{(i)}} c_l^{(j)} + \sqrt{(1 - \epsilon_i)\epsilon_j} \sum_{l=0}^{n_{\text{dim}}-1} G_{j+n_{\text{dim}},l} c_l^{(i)} \\
& + \sqrt{\epsilon_i(1 - \epsilon_j)} \sum_{l=0}^{n_{\text{dim}}-1} \overline{c_l^{(j)}} G_{l,i+n_{\text{dim}}} + \sqrt{\epsilon_i\epsilon_j} G_{i+n_{\text{dim}},j+n_{\text{dim}}}, \quad \forall i, j, \\
& \text{Tr}[(|j\rangle\langle j|_A \otimes \Gamma_k) \rho_{AB}] = p_j Y_{k|j}, \quad \forall j, k, \\
& G_{m,m} = 1, \quad \forall m \in \{0, \dots, n_{\text{dim}} + n - 1\}, \\
& G_{l,l'} = 0, \quad \forall l, l' \in \{0, \dots, n_{\text{dim}} - 1\}, l \neq l', \\
& \sum_{l=0}^{n_{\text{dim}}-1} G_{j+n_{\text{dim}},l} c_l^{(j)} = 0, \quad \forall j, \\
& (h, \rho_{AB}) \in \mathcal{K}_{\text{QKD}}^{\mathcal{G}, \mathcal{Z}} \\
& G \succeq 0.
\end{aligned} \tag{B5}$$

We remark that an analogous approach can be applied to the optimization problem for MDI-type protocols in Appendix C to handle the scenario in which the joint reference states $\{|\phi_{ij}\rangle\}_{i,j}$ are linearly dependent.

Appendix C: Optimization problem for MDI-type protocols

Here, we explain how to construct the optimization problem for MDI-type protocols, starting with the case of full state characterization, where Alice's and Bob's emitted states are completely known. We then show how to extend this construction to the scenario of partial state characterization.

1. Full state characterization

Consider a general MDI-type QKD protocol in which, for each round, Alice independently selects a setting $i \in \{0, \dots, n_A - 1\}$ with probability p_i^A and emits state $|\psi_i^A\rangle$, while Bob independently selects a setting $j \in \{0, \dots, n_B - 1\}$ with probability p_j^B and emits state $|\psi_j^B\rangle$. The joint quantum state sent to Eve is therefore $|\psi_{ij}\rangle = |\psi_i^A\rangle \otimes |\psi_j^B\rangle$, selected with probability $p_{ij} = p_i^A p_j^B$. To prove security, we employ the source replacement scheme where Alice and Bob generate the entangled state

$$|\Psi\rangle_{ABA'B'} = \sum_{i,j} \sqrt{p_{ij}} |ij\rangle_{AB} |\psi_{ij}\rangle_{A'B'}, \tag{C1}$$

where A (B) is an ancillary system that Alice (Bob) retains, and A' (B') is the photonic system sent through the quantum channel.

In MDI protocols, Eve performs a joint measurement on the incoming systems and announces a classical outcome. This can be described by an isometry $V_{A'B' \rightarrow CE}$, where C is a classical register containing Eve's announcement and E is Eve's quantum side information. Since we are interested in the reduced state ρ_{ABC} that Alice and Bob share after Eve's announcement, we can define a CPTP map $\mathcal{E}_{A'B' \rightarrow C}$ that consists of first applying $V_{A'B' \rightarrow CE}$ and then tracing out system E , obtaining

$$\rho_{ABC} = (\mathcal{I}_{AB} \otimes \mathcal{E}_{A'B' \rightarrow C})(|\Psi\rangle\langle\Psi|_{ABA'B'}). \tag{C2}$$

Since C is classical, we can decompose the state as

$$\rho_{ABC} = \sum_{\gamma} \rho_{AB}^{(\gamma)} \otimes |\gamma\rangle\langle\gamma|_C, \tag{C3}$$

where γ indexes Eve's possible announcements and $\rho_{AB}^{(\gamma)}$ represents the (subnormalized) conditional state of Alice and Bob's systems given announcement γ .

The asymptotic SKR for MDI protocols follows Eq. (4) from the main text, but now involves optimizing over the family of subnormalized states $\{\rho_{AB}^{(\gamma)}\}_{\gamma}$:

$$\begin{aligned} & \min_{\{\rho_{AB}^{(\gamma)}\}_{\gamma}} D(\mathcal{G}(\rho_{ABC}) \| \mathcal{Z}(\mathcal{G}(\rho_{ABC}))) \\ & \text{s.t. } \rho_{ABC} = \sum_{\gamma} \rho_{AB}^{(\gamma)} \otimes |\gamma\rangle\langle\gamma|_C, \\ & \sum_{\gamma} \langle ij | \rho_{AB}^{(\gamma)} | i'j' \rangle = \sqrt{p_{ij}p_{i'j'}} \langle \psi_{i'j'} | \psi_{ij} \rangle, \quad \forall i, i', j, j', \\ & \text{Tr}[|ij\rangle\langle ij|_{AB} \rho_{AB}^{(\gamma)}] = p_{ij} Y_{\gamma|ij}, \quad \forall i, j, \gamma, \\ & \rho_{AB}^{(\gamma)} \succeq 0, \quad \forall \gamma. \end{aligned} \quad (\text{C4})$$

The second constraint is equivalent to

$$\rho_{AB} := \text{Tr}_C[\rho_{ABC}] = \sum_{\gamma} \rho_{AB}^{(\gamma)} = \text{Tr}_{A'B'}[|\Psi\rangle\langle\Psi|_{ABA'B'}], \quad (\text{C5})$$

and comes from the fact that Eve's map does not act on systems AB (see Eq. (C2)), and therefore the marginal state on AB must be the same before and after Eve applies her map. The third constraint in Eq. (C4) comes from Alice and Bob's observations during protocol execution, where $Y_{\gamma|ij}$ refers to the conditional probability that Eve announces outcome γ given that Alice selects setting i and Bob selects setting j . The remaining constraints ensure that ρ_{ABC} is properly normalized and positive semidefinite.

As in the main text, following the approach in [18], this can be reformulated as the conic optimization problem:

$$\begin{aligned} & \min_{h, \{\rho_{AB}^{(\gamma)}\}_{\gamma}} h \\ & \text{s.t. } \rho_{ABC} = \sum_{\gamma} \rho_{AB}^{(\gamma)} \otimes |\gamma\rangle\langle\gamma|_C, \\ & \sum_{\gamma} \langle ij | \rho_{AB}^{(\gamma)} | i'j' \rangle = \sqrt{p_{ij}p_{i'j'}} \langle \psi_{i'j'} | \psi_{ij} \rangle, \quad \forall i, i', j, j', \\ & \text{Tr}[|ij\rangle\langle ij|_{AB} \rho_{AB}^{(\gamma)}] = p_{ij} Y_{\gamma|ij}, \quad \forall i, j, \gamma, \\ & (h, \rho_{ABC}) \in \mathcal{K}_{\text{QKD}}^{\widehat{\mathcal{G}}, \widehat{\mathcal{Z}}}. \end{aligned} \quad (\text{C6})$$

2. Partial state characterization

Now consider the realistic scenario where Alice and Bob only have partial knowledge of their emitted states. Specifically, they only know that their joint state $\rho_{ij} = \rho_i \otimes \rho_j$, emitted when they select settings i and j , respectively, satisfies

$$\langle \phi_{ij} | \rho_{ij} | \phi_{ij} \rangle \geq 1 - \varepsilon_{ij}, \quad (\text{C7})$$

where $\{|\phi_{ij}\rangle\}_{ij}$ are known reference states and $\{\varepsilon_{ij}\}_{ij}$ are known deviation bounds s.t. $0 \leq \varepsilon_{ij} \leq 1$. Following Section A, we can assume, without loss of generality, that the joint emitted states are pure, i.e. $\rho_{ij} = |\psi_{ij}\rangle\langle\psi_{ij}|$, and have the form

$$|\psi_{ij}\rangle = \sqrt{1 - \varepsilon_{ij}} |\phi_{ij}\rangle + \sqrt{\varepsilon_{ij}} |\phi_{ij}^{\perp}\rangle, \quad (\text{C8})$$

where $|\phi_{ij}^{\perp}\rangle$ are unknown states orthogonal to the reference states: $\langle \phi_{ij}^{\perp} | \phi_{ij} \rangle = 0$.

The key insight from the main text, i.e., that the optimization depends only on inner products between states, applies directly to the MDI case as well. We introduce a Gram matrix G containing all inner products between the states in

$\{|\phi_{ij}\rangle\}_{ij} \cup \{|\phi_{ij}^\perp\rangle\}_{ij}$. This is a $(2n_A n_B \times 2n_A n_B)$ positive semidefinite matrix:

$$G = \begin{pmatrix} \langle \phi_{00} | \phi_{00} \rangle & \langle \phi_{00} | \phi_{01} \rangle & \cdots & \langle \phi_{00} | \phi_{00}^\perp \rangle & \langle \phi_{00} | \phi_{01}^\perp \rangle & \cdots \\ \langle \phi_{01} | \phi_{00} \rangle & \langle \phi_{01} | \phi_{01} \rangle & \cdots & \langle \phi_{01} | \phi_{00}^\perp \rangle & \langle \phi_{01} | \phi_{01}^\perp \rangle & \cdots \\ \vdots & \vdots & \ddots & \vdots & \vdots & \ddots \\ \langle \phi_{00}^\perp | \phi_{00} \rangle & \langle \phi_{00}^\perp | \phi_{01} \rangle & \cdots & \langle \phi_{00}^\perp | \phi_{00}^\perp \rangle & \langle \phi_{00}^\perp | \phi_{01}^\perp \rangle & \cdots \\ \langle \phi_{01}^\perp | \phi_{00} \rangle & \langle \phi_{01}^\perp | \phi_{01} \rangle & \cdots & \langle \phi_{01}^\perp | \phi_{00}^\perp \rangle & \langle \phi_{01}^\perp | \phi_{01}^\perp \rangle & \cdots \\ \vdots & \vdots & \ddots & \vdots & \vdots & \ddots \end{pmatrix}, \quad (\text{C9})$$

where each index pair (ij) for each subblock runs over all $n_A \times n_B$ combinations of Alice's and Bob's settings. Note that some entries of G are known, while others are unknown. More specifically, the known entries are: the entire upper left subblock (since the states $\{|\phi_{ij}\rangle\}_{ij}$ are known), all the diagonal entries (since all the states are normalized), and all the entries of the form $\langle \phi_{ij}^\perp | \phi_{ij} \rangle$ (which are equal to zero). Thus, by introducing G as an optimization variable constrained by this known information, we can reformulate the optimization problem with partial state characterization as a conic problem. For MDI protocols with partial state characterization, this problem becomes

$$\begin{aligned} & \min_{h, \{\rho_{AB}^{(\gamma)}\}_\gamma, G} h \\ \text{s.t. } & \rho_{ABC} = \sum_\gamma \rho_{AB}^{(\gamma)} \otimes |\gamma\rangle\langle\gamma|_C, \\ \frac{\langle ij | \rho_{AB}^{(\gamma)} | i'j' \rangle}{\sqrt{p_{ij} p_{i'j'}}} &= \sum_{a,b \in \{0,1\}} \sqrt{\varepsilon_{ij}^a (1 - \varepsilon_{ij})^{1-a} \varepsilon_{i'j'}^b (1 - \varepsilon_{i'j'})^{1-b}} G_{(ij,a), (i'j',b)}, \\ \text{Tr}[|ij\rangle\langle ij|_{AB} \rho_{AB}^{(\gamma)}] &= p_{ij} Y_{\gamma|ij}, \quad \forall i, j, \gamma, \\ G_{(ij,0), (ij,0)} &= 1, \quad G_{(ij,1), (ij,1)} = 1, \quad G_{(ij,0), (ij,1)} = 0, \quad \forall i, j, \\ G_{(ij,0), (i'j',0)} &= \langle \phi_{ij} | \phi_{i'j'} \rangle, \quad \forall (ij) \neq (i'j'), \\ (h, \rho_{ABC}) &\in \mathcal{K}_{\text{QKD}}^{\widehat{\mathcal{G}}, \widehat{\mathcal{Z}}}, \quad G \succeq 0. \end{aligned} \quad (\text{C10})$$

where, for notational convenience, we have indexed the matrix G using pairs (ij, a) for $a \in \{0, 1\}$, with $a = 0$ corresponding to $|\phi_{ij}\rangle$ and $a = 1$ to $|\phi_{ij}^\perp\rangle$.

Appendix D: Protocol modeling

Here, we explain how to model and simulate the SKR for the BB84 protocol and the coherent-light-based MDI protocol introduced in [7], which are considered in the numerical simulations presented in the main text.

1. BB84 protocol

Since this is a prepare-and-measure protocol, we use the conic optimization problem in Eq. (12). In this protocol, Alice sends four different states indexed by $j \in \{0, 1, 2, 3\}$, which correspond to the bit-and-basis values $\{0_Z, 1_Z, 0_X, 1_X\}$, respectively, and are selected with probabilities

$$p_0 = p_1 = p_{Z_A}/2 \quad \text{and} \quad p_2 = p_3 = p_{X_A}/2, \quad (\text{D1})$$

with $p_{X_A} = 1 - p_{Z_A}$. The reference states $|\phi_j\rangle$ are given by Eq. (13), from which all the inner products $\langle \phi_{j'} | \phi_j \rangle$ can be directly calculated.

As for Bob, we consider that he performs an active basis choice, although our approach can equally be applied to setups in which he performs a passive basis choice, e.g., using a 50:50 beam splitter to divide the incoming signal. In an active basis choice setup, Bob chooses between the Z basis or the X basis measurement with probability p_{Z_B} and $p_{X_B} = 1 - p_{Z_B}$, respectively, and performs the selected measurement, obtaining either a bit value or an inconclusive outcome. Since the focus of our work is on source imperfections, we assume that Bob's detectors are identical, and that the only non-idealities of his measurement setup are: (1) non-unity detector efficiencies and (2) dark counts. For

attempts to incorporate partially characterized imperfections in Bob's setup into numerical security proofs such as ours, we refer the reader to Ref. [26].

Bob's Z and X POVMs can be described by $\{\Gamma_0^{(Z)}, \Gamma_1^{(Z)}, \Gamma_{\perp}\}$ and $\{\Gamma_0^{(X)}, \Gamma_1^{(X)}, \Gamma_{\perp}\}$, respectively. However, in our model, Bob performs a single POVM $\{\Gamma_k\}_k$. This is not a problem, since we can regard Bob's overall action as a five outcome POVM $\{\Gamma_{0Z}, \Gamma_{1Z}, \Gamma_{0X}, \Gamma_{1X}, \Gamma_{\perp}\}$, where

$$\Gamma_{0Z} = p_{Z_B} \Gamma_0^{(Z)}, \quad \Gamma_{1Z} = p_{Z_B} \Gamma_1^{(Z)}, \quad \Gamma_{0X} = p_{X_B} \Gamma_0^{(X)}, \quad \Gamma_{1X} = p_{X_B} \Gamma_1^{(X)} \quad \text{and} \quad \Gamma_{\perp} = \mathbb{I} - \Gamma_{0Z} - \Gamma_{1Z} - \Gamma_{0X} - \Gamma_{1X}. \quad (\text{D2})$$

Note that, in reality, Bob's POVM acts on an infinitely-dimensional system, since Eve can resend to Bob any number of photons she wishes. However, for an active BB84 setup in which Bob's detectors are identical, we can apply the qubit squasher [24, 25]. Moreover, we can consider without loss of generality that any non-unit efficiency in Bob's detectors is part of the quantum channel, and their dark counts can be regarded as channel-induced noise (see [26] for a proof of this). Thus, we can consider that Bob's POVM is ideal and acts on a three-dimensional system with orthonormal basis $\{|0\rangle_B, |1\rangle_B, |2\rangle_B\}$, where $|0\rangle_B$ ($|1\rangle_B$) corresponds to a single-photon with horizontal (vertical) encoding, and $|2\rangle_B$ corresponds to no photon. In particular, we can consider Bob's POVM elements to be

$$\Gamma_{0Z} = p_{Z_B} |0\rangle\langle 0|_B, \quad \Gamma_{1Z} = p_{Z_B} |1\rangle\langle 1|_B, \quad \Gamma_{0X} = p_{X_B} |+\rangle\langle +|_B, \quad \Gamma_{1X} = p_{X_B} |-\rangle\langle -|_B \quad \text{and} \quad \Gamma_{\perp} = |2\rangle\langle 2|_B, \quad (\text{D3})$$

where we have defined $|\pm\rangle_B = (|0\rangle_B \pm |1\rangle_B)/\sqrt{2}$.

Now, we define the maps \mathcal{G} and \mathcal{Z} , which specify the filtered state from which the sifted key is extracted, and how Alice extracts her sifted key bits, respectively. Here, we consider the efficient version of the BB84 protocol, in which Alice and Bob use the Z basis most of the time, and extract the key only from this basis. This maximizes the sifting efficiency, and is thus expected to result in higher SKRs. We remark, however, that our technique also directly applies to the case in which Alice and Bob extract key from both bases, for any values of p_{Z_A} and p_{Z_B} .

Since the sifted key is extracted from the events in which Alice selects $j = 0$ or $j = 1$ and Bob obtains $k = 0Z$ or $k = 1Z$, the map \mathcal{G} has the form

$$\mathcal{G}(\rho) = G\rho G, \quad (\text{D4})$$

where

$$G = \sqrt{(|0\rangle\langle 0|_A + |1\rangle\langle 1|_A) \otimes (\Gamma_{0Z} + \Gamma_{1Z})} = \sqrt{p_{Z_B}} (|0\rangle\langle 0|_A + |1\rangle\langle 1|_A) \otimes (|0\rangle\langle 0|_B + |1\rangle\langle 1|_B). \quad (\text{D5})$$

On the other hand, since Alice assigns bit “0” when $j = 0$ and bit “1” when $j = 1$, the map \mathcal{Z} has the form

$$\mathcal{Z}(\sigma) = Z_0\sigma Z_0 + Z_1\sigma Z_1, \quad (\text{D6})$$

where

$$Z_0 = |0\rangle\langle 0|_A \otimes (|0\rangle\langle 0|_B + |1\rangle\langle 1|_B) \quad \text{and} \quad Z_1 = |1\rangle\langle 1|_A \otimes (|0\rangle\langle 0|_B + |1\rangle\langle 1|_B). \quad (\text{D7})$$

As explained in Ref. [18], in order to use those maps in the conic problem in Eq. (12), we need to perform facial reduction on them, that is, find strictly positive maps $\widehat{\mathcal{G}}, \widehat{\mathcal{Z}}$ such that $\mathcal{G}(\rho) = V\widehat{\mathcal{G}}(\rho)V^\dagger$ and $\mathcal{Z} \circ \mathcal{G}(\rho) = W\widehat{\mathcal{Z}}(\rho)W^\dagger$ for some isometries V and W . A straightforward calculation shows that the following maps satisfy this: $\widehat{\mathcal{G}}(\rho) := V^\dagger \mathcal{G}(\rho) V$ and $\widehat{\mathcal{Z}}(\rho) := W^\dagger (\mathcal{Z} \circ \mathcal{G}(\rho)) W$ for $V = W = (|0\rangle_A \langle 0|_{A'} + |1\rangle_A \langle 1|_{A'}) \otimes (|0\rangle_B \langle 0|_{B'} + |1\rangle_B \langle 1|_{B'})$, where $\{|0\rangle_{A'}, |1\rangle_{A'}\}$ and $\{|0\rangle_{B'}, |1\rangle_{B'}\}$ are orthonormal bases of dimension 2, instead of the original dimensions 4 and 3, respectively.

The only remaining undefined terms in Eq. (12) and the key rate formula in Eq. (4) are the yield probabilities $Y_{k|j}$, the probability that a round is used for key generation

$$p_{\text{pass}} = \frac{p_{Z_A}}{2} (Y_{Z0|0} + Y_{Z0|1} + Y_{Z1|0} + Y_{Z1|1}), \quad (\text{D8})$$

and the cost of error correction per sifted key bit λ_{EC} . In a real implementation, these terms would be observed during the protocol execution. Instead, here we estimate them using the channel model below.

Note: Although the approach described in this section is valid for any $p_{Z_A}, p_{Z_B} \in (0, 1)$ the asymptotic key rate is achieved in the limit $p_{Z_A}, p_{Z_B} \rightarrow 1$. While this limit can be directly implemented in Eqs. (D5) and (D8) by setting $p_{Z_A} = p_{Z_B} = 1$, setting $p_{X_A} = p_{X_B} = 0$ in Eqs. (D1), (D3) and (12) leads to divisions by zero and loss of constraints. To circumvent this issue, we simultaneously set $p_{Z_A} = p_{Z_B} = 1$ and $p_{X_A} = p_{X_B} = 1$ throughout the

optimization. While this results in an unphysical scenario with $\text{Tr}[\rho_{AB}] = 2$, the optimization problem remains well-defined and correctly recovers the asymptotic key rate. This approach was used to generate the results in the main text.

Channel model

We consider a standard BB84 channel model with a lossy channel and an active-basis receiver. The overall transmission efficiency is $\eta = \eta_c \eta_d$ with channel transmission $\eta_c = 10^{-0.02l}$ (for channel length l in km) and detector efficiency η_d . The dark-count probability is denoted by p_d , and for simplicity we assume no channel misalignment. By neglecting $O(p_d^2)$ terms, we can express the yields as

$$\begin{aligned} Y_{Z0|j} &= p_{Z_B} \left((1 - \eta) p_d + \frac{\eta}{2} \left[1 + (1 - p_d) \cos(2\theta_j) \right] \right), \\ Y_{Z1|j} &= p_{Z_B} \left((1 - \eta) p_d + \frac{\eta}{2} \left[1 - (1 - p_d) \cos(2\theta_j) \right] \right), \\ Y_{X0|j} &= p_{X_B} \left((1 - \eta) p_d + \frac{\eta}{2} \left[1 + (1 - p_d) \sin(2\theta_j) \right] \right), \\ Y_{X1|j} &= p_{X_B} \left((1 - \eta) p_d + \frac{\eta}{2} \left[1 - (1 - p_d) \sin(2\theta_j) \right] \right), \end{aligned} \quad (\text{D9})$$

where $Y_{B\beta|j}$ denotes the probability that Bob selects basis $B \in \{Z, X\}$ and obtains bit outcome $\beta \in \{0, 1\}$, conditioned on Alice having selected setting j . As discussed in the main text, we set $\theta_j = (1 + \delta/\pi) \varphi_j/2$, with $\varphi_j \in \{0, \pi, \pi/2, 3\pi/2\}$ corresponding to $j \in \{0, 1, 2, 3\}$, where $\delta \in [0, \pi)$ quantifies the magnitude of the state preparation flaws.

As for the cost of error correction, we assume that $\lambda_{\text{EC}} = f h(e_Z)$, where f is the error correction inefficiency, $h(x) = -x \log_2 x - (1 - x) \log_2(1 - x)$ is the binary entropy function, and e_Z is the bit-error rate, which is calculated from the yields in Eq. (D9) as

$$e_Z = \frac{Y_{Z1|0} + Y_{Z0|1}}{Y_{Z0|0} + Y_{Z1|0} + Y_{Z0|1} + Y_{Z1|1}}. \quad (\text{D10})$$

2. Coherent-light-based MDI protocol

In the coherent-light-based MDI protocol in [7], Alice and Bob ideally prepare the states $\{|\alpha\rangle, |-\alpha\rangle, |\text{vac}\rangle\}$, where $|\alpha\rangle$ and $|-\alpha\rangle$ are coherent states with opposite phases (used for key generation), and $|\text{vac}\rangle$ is a vacuum state (used only for parameter estimation). We model characterized state preparation flaws by considering that one of the emitted coherent states is shifted by an angle δ . That is, for each user, we consider the reference states

$$|\phi_0\rangle = |\alpha\rangle, \quad |\phi_1\rangle = |-\alpha e^{i\delta}\rangle \quad \text{and} \quad |\phi_2\rangle = |\text{vac}\rangle, \quad (\text{D11})$$

with the joint reference states given by $|\phi_{ij}\rangle = |\phi_i\rangle \otimes |\phi_j\rangle$. The inner products $\langle \phi_{i'j'} | \phi_{ij} \rangle$ can then be calculated directly. We consider that the state emission probabilities are $p_0 = p_1 = p^c/2$ and $p_2 = 1 - p^c$, where p^c is the probability that the users select a coherent state and each coherent state is selected equally likely. The joint selection probabilities are thus $p_{ij} = p_i p_j$ for $i, j \in \{0, 1, 2\}$.

If Charlie is honest, he interferes the two incoming signals at a 50:50 beam splitter, followed by threshold detectors D_c and D_d placed at the output ports corresponding to constructive and destructive interference, respectively. He then announces the result $\gamma = 0$ if only detector D_c clicks, $\gamma = 1$ if only detector D_d clicks, or $\gamma = 2$ if neither detector clicks or both detectors click. Of course, Charlie may be dishonest, and even controlled by Eve, so they may select the announcements using any measurement and strategy they see fit.

Note that, in the MDI case, no squashing map is needed since Alice and Bob's systems A and B are both guaranteed to be finite dimensional, since they are fictitious ancillary systems kept in their labs.

Alice and Bob extract their sifted key from the rounds in which $i, j \in \{0, 1\}$ and $\gamma \in \{0, 1\}$, with $i = 0$ or $j = 0$ corresponding to bit 0 and $i = 1$ or $j = 1$ corresponding to bit 1. For the rounds in which $\gamma = 1$, Bob flips his sifted key bit, since destructive interference should indicate anticorrelation between Alice's and Bob's coherent states. The maps \mathcal{G} and \mathcal{Z} are thus given by

$$\mathcal{G}(\rho) = G \rho G, \quad \text{with } G = (|0\rangle\langle 0|_A + |1\rangle\langle 1|_A) \otimes (|0\rangle\langle 0|_B + |1\rangle\langle 1|_B) \otimes (|0\rangle\langle 0|_C + |1\rangle\langle 1|_C), \quad (\text{D12a})$$

$$\mathcal{Z}(\sigma) = Z_0 \sigma Z_0 + Z_1 \sigma Z_1, \quad \text{with } Z_j = |j\rangle\langle j|_A \otimes (|0\rangle\langle 0|_B + |1\rangle\langle 1|_B) \otimes (|0\rangle\langle 0|_C + |1\rangle\langle 1|_C) \text{ for } j \in \{0, 1\}. \quad (\text{D12b})$$

For a more efficient optimization, we now use the decomposition (C3) to simplify these maps. Applying them to ρ_{ABC} we get

$$\mathcal{G}(\rho_{ABC}) = \sum_{\gamma=0}^1 \mathcal{G}'(\rho_{AB}^{(\gamma)}) \otimes |\gamma\rangle\langle\gamma|_C, \quad (\text{D13a})$$

$$\mathcal{Z} \circ \mathcal{G}(\rho_{ABC}) = \sum_{\gamma=0}^1 \mathcal{Z}'(\rho_{AB}^{(\gamma)}) \otimes |\gamma\rangle\langle\gamma|_C, \quad (\text{D13b})$$

where

$$\mathcal{G}'(\rho) = G' \rho G', \text{ with } G' = (|0\rangle\langle 0|_A + |1\rangle\langle 1|_A) \otimes (|0\rangle\langle 0|_B + |1\rangle\langle 1|_B), \quad (\text{D14a})$$

$$\mathcal{Z}'(\sigma) = Z'_0 \sigma Z'_0 + Z'_1 \sigma Z'_1, \text{ with } Z'_j = |j\rangle\langle j|_A \otimes (|0\rangle\langle 0|_B + |1\rangle\langle 1|_B) \text{ for } j \in \{0, 1\}. \quad (\text{D14b})$$

Now, we use the fact that $D(\sum_i \rho_i \otimes |i\rangle\langle i| \parallel \sum_i \sigma_i \otimes |i\rangle\langle i|) = \sum_i D(\rho_i \parallel \sigma_i)$ and conclude that

$$D(\mathcal{G}(\rho_{ABC}) \parallel \mathcal{Z} \circ \mathcal{G}(\rho_{ABC})) = \sum_{\gamma=0}^1 D(\mathcal{G}'(\rho_{AB}^{(\gamma)}) \parallel \mathcal{Z}'(\rho_{AB}^{(\gamma)})), \quad (\text{D15})$$

which allows us to break down the relative entropy optimization into two cones of lower dimension. As in the BB84 case, we now need to do facial reduction on the maps $\mathcal{G}', \mathcal{Z}'$. Let then $V = (|0\rangle_A \langle 0|_{A'} + |1\rangle_A \langle 1|_{A'}) \otimes (|0\rangle_B \langle 0|_{B'} + |1\rangle_B \langle 1|_{B'})$, where $\{|0\rangle_{A'}, |1\rangle_{A'}\}$ and $\{|0\rangle_{B'}, |1\rangle_{B'}\}$ are orthonormal bases of dimension 2, instead of the original 3. Then $\widehat{\mathcal{G}}(\rho) := V^\dagger \mathcal{G}'(\rho) V$ and $\widehat{\mathcal{Z}}(\rho) := V^\dagger \mathcal{Z}'(\rho) V$ are strictly positive and respect $\mathcal{G}'(\rho) = V \widehat{\mathcal{G}}(\rho) V^\dagger$ and $\mathcal{Z}'(\rho) = V \widehat{\mathcal{Z}}(\rho) V^\dagger$, as required.

The remaining terms in the optimization program in Eq. (C10) and the key rate formula in Eq. (4) are the yield probabilities $Y_{\gamma|ij}$, the probability that a round is used for key generation

$$p_{\text{pass}} = \sum_{i,j \in \{0,1\}} p_{ij} (Y_{0|ij} + Y_{1|ij}), \quad (\text{D16})$$

and the cost of error correction per sifted key bit λ_{EC} . In a real implementation, these terms would be observed during the protocol execution. Instead, here we estimate them using the channel model below.

Note: Similarly to the BB84 protocol, the approach described in this section is valid for any $p^c \in (0, 1)$. However, the asymptotic key rate is achieved in the limit $p^c \rightarrow 1$ and $p_2 = 1 - p^c \rightarrow 0$. While this limit can be directly implemented in Eq. (D16), setting $p_2 = 0$ in Eq. (C10) leads to divisions by zero and loss of constraints. To circumvent this issue, one can simultaneously set $p^c = 1$ and $p_2 = 1$ throughout the optimization. While this results in an unphysical scenario with $\text{Tr}[\rho_{ABC}] = 4$, the optimization problem remains well-defined and correctly recovers the asymptotic key rate. Equivalently, one can set $p^c = 2/3$ and $p_2 = 1/3$ and multiply the result by $9/4$. We used the latter approach to generate the results in the main text and in Section F.

Channel model

We model the links from Alice and Bob to Charlie as independent lossy channels with transmittance η . For simplicity, we assume that both detectors at Charlie's have a dark-count probability p_d . Recall that Charlie announces $\gamma = 0$ if detector D_c clicks and detector D_d does not click, $\gamma = 1$ if detector D_c does not click and detector D_d clicks, and $\gamma = 2$ otherwise. Under these assumptions, the yields $Y_{\gamma|ij}$ can be expressed as

$$\begin{aligned} Y_{0|ij} &= \left[1 - \exp\left(-\frac{\eta}{2} |\phi_i + \phi_j|^2\right) (1 - p_d) \right] \exp\left(-\frac{\eta}{2} |\phi_i - \phi_j|^2\right) (1 - p_d), \\ Y_{1|ij} &= \left[1 - \exp\left(-\frac{\eta}{2} |\phi_i - \phi_j|^2\right) (1 - p_d) \right] \exp\left(-\frac{\eta}{2} |\phi_i + \phi_j|^2\right) (1 - p_d), \end{aligned} \quad (\text{D17})$$

and $Y_{2|ij} = 1 - Y_{0|ij} - Y_{1|ij}$. The parameters ϕ_i in Eq. (D17) represent the complex amplitudes of the coherent states, with values $\phi_0 = \alpha$, $\phi_1 = -\alpha e^{i\delta}$, and $\phi_2 = 0$, where $\delta \in [0, \pi]$ quantifies the magnitude of the state preparation flaws.

As for the cost of error correction, we assume that $\lambda_{\text{EC}} = fh(e_{\text{bit}})$, where f is the error correction inefficiency, $h(x) = -x \log_2 x - (1 - x) \log_2(1 - x)$ is the binary entropy function, and e_{bit} is the bit-error rate, which can be

defined directly from the yields in Eq. (D17) as

$$e_{\text{bit}} = \frac{\sum_{(i,j) \in \mathcal{S}_{\text{diff}}} Y_{0|i,j} + \sum_{(i,j) \in \mathcal{S}_{\text{same}}} Y_{1|i,j}}{\sum_{(i,j) \in \mathcal{S}_{\text{same}} \cup \mathcal{S}_{\text{diff}}} (Y_{0|i,j} + Y_{1|i,j})}, \quad (\text{D18})$$

where $\mathcal{S}_{\text{same}} = \{(0,0), (1,1)\}$ and $\mathcal{S}_{\text{diff}} = \{(0,1), (1,0)\}$.

Appendix E: Reconstructing solution

Here, we show that the Gram matrix formulation of the phase-error rate estimation in [20] is not a relaxation, but an equivalent formulation. We do this by showing that given a positive semidefinite Gram matrix G respecting the constraints, we can reconstruct measurement operators M_γ and states $|\phi_j\rangle, |\phi_j^\perp\rangle$ that reproduce the entries of G .

Since G is positive semidefinite, there exists a matrix V such that $V^\dagger V = G$. The columns of V are the vectors $|M_\gamma \phi_j\rangle, |M_\gamma \phi_j^\perp\rangle$ that give the desired inner products. We need then to find $M_\gamma, |\phi_j\rangle, |\phi_j^\perp\rangle$ such that $M_\gamma |\phi_j\rangle = |M_\gamma \phi_j\rangle$ and $M_\gamma |\phi_j^\perp\rangle = |M_\gamma \phi_j^\perp\rangle$.

Let then g_γ be the principal submatrix of G containing the rows and columns corresponding to $|M_\gamma \phi_j\rangle, |M_\gamma \phi_j^\perp\rangle$ for all j . Since they are principal submatrices of a positive semidefinite matrix, they are also positive semidefinite. Now let $g = \sum_\gamma g_\gamma$. It is also positive semidefinite, and therefore there exists W such that $W^\dagger W = G$. Let $|\phi_j\rangle, |\phi_j^\perp\rangle$ be the columns of W . We have that $\langle \phi_j^{(\perp)} | \phi_i^{(\perp)} \rangle = \sum_\gamma \langle M_\gamma \phi_j^{(\perp)} | M_\gamma \phi_i^{(\perp)} \rangle$, and therefore the inner products between the reconstructed vectors obey the constraints imposed on G .

It remains to reconstruct the measurement operators M_γ . This amounts to solving the linear systems $M_\gamma |\phi_j\rangle = |M_\gamma \phi_j\rangle$ and $M_\gamma |\phi_j^\perp\rangle = |M_\gamma \phi_j^\perp\rangle$ over M_γ , or equivalently $M_\gamma W = V_\gamma$, where V_γ contains the columns of V associated to index γ . To do this we need a more careful construction of W . Let an eigendecomposition of g be $\sum_j \lambda_j |v_j\rangle\langle v_j|$, and define

$$W = \sum_{j; \lambda_j > 0} \sqrt{\lambda_j} |j\rangle\langle v_j|, \quad (\text{E1})$$

where $\{|j\rangle\}$ is an orthonormal basis of dimension $\text{rank}(g)$. This particular choice of W has a right inverse

$$W^R = \sum_{j; \lambda_j > 0} \frac{1}{\sqrt{\lambda_j}} |v_j\rangle\langle j|, \quad (\text{E2})$$

and for all γ we can define $M_\gamma = V_\gamma W^R$.

Appendix F: Additional simulations

Here, we investigate the SKR of the coherent-light-based MDI protocol when $\delta = 0$ and $p_d = 10^{-4}$. The results shown in Fig. 3 indicate that, in this regime, there is also a clear difference between the two approaches, with our method outperforming that in [20].

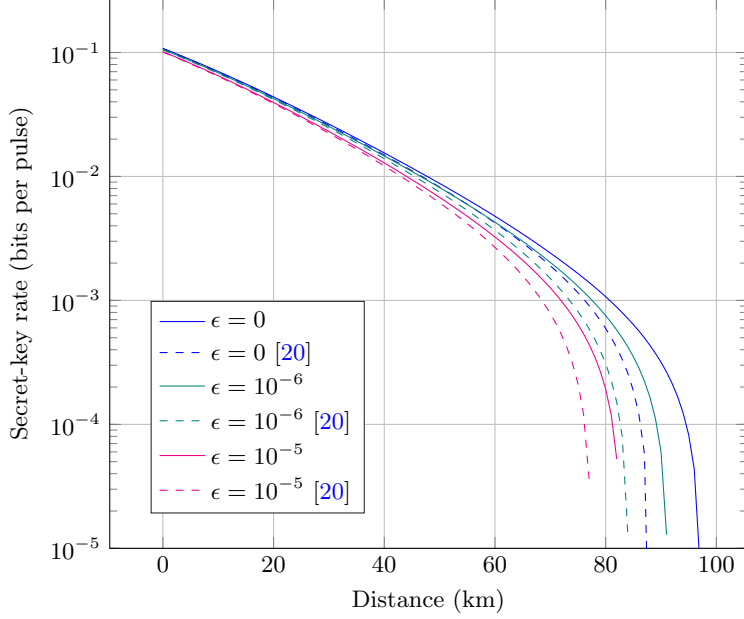


Figure 3. Secret-key rate (logarithmic scale) as a function of distance for the coherent-light-based MDI protocol with $\delta = 0$, $p_d = 10^{-4}$ and different values of ϵ (which accounts for both Alice's and Bob's source imperfections). The solid lines correspond to our conic optimization approach while the dashed lines correspond to the phase-estimation method of [20]. The parameter α has been optimized for each distance point, taking values roughly in the range $[0.1, 0.4]$. All computations were performed with double floats for increased precision and stability.